the line width data, as discussed above. It should also be possible to determine χ if the complete field dependence of each OTf-bound ^{27}Al signal is known; such work is currently in progress.

A number of studies have already shown that quadrupolar nuclei bound to small proteins may be monitored successfully by NMR spectroscopy. For example, the binding of Ca^{2+} to several calcium-binding proteins has been investigated using ^{43}Ca NMR.[54,55] This study demonstrates the feasibility of using ^{27}Al NMR to probe Al^{3+} binding to much larger proteins such as transferrins. In principle, this methodology may be extended to other metal-binding proteins and to other metal ions which have NMR-observable quadrupolar nuclei. However, as shown in this work and

by Butler and Eckert,[14] the detectability of the central transition of quadrupolar nuclei bound to large proteins hinges considerably on a number of factors which are to some extent in the control of the experimentor and must be chosen with great care: (1) the strength of the external magnetic field (ω_0), (2) the size and motion of the macromolecule in question (τ_c, temperature, solution viscosity), (3) the intrinsic quadrupole moment of the specific nucleus (Q), and (4) the nature of the electric field gradient at the metal ion binding site.

(54) Vogel, H. J.; Forsén, S. In *Biological Magnetic Resonance*; Berliner, L. J., Reuben, J., Eds.; Plenum Press: New York, 1987; Vol. 7, pp 249-309.
(55) Aramini, J. M.; Drakenberg, T.; Hiraoki, T.; Ke, Y.; Nitta, K.; Vogel, H. J. *Biochemistry* **1992**, *31*, 6761-6768.

Determination of the Nitrogen Chemical Structures in Petroleum Asphaltenes Using XANES Spectroscopy

Sudipa Mitra-Kirtley,[†,‡] Oliver C. Mullins,*[,†] Jan van Elp,[‡] Simon J. George,[§] Jie Chen,[‡] and Stephen P. Cramer[‡,§]

Contribution from Schlumberger-Doll Research, Ridgefield, Connecticut 06877, Lawrence Berkeley Laboratory, Berkeley, California 94720, and University of California, Davis, California 95616. Received July 23, 1992

Abstract: Extensive nitrogen K-edge X-ray absorption studies have been performed for the first time on seven petroleum asphaltenes and nitrogen standard compounds for the purpose of determining chemical forms of nitrogen present in the asphaltenes; such an objective is difficult to achieve by any other method. Sulfur XANES studies on fossil fuel samples have provided a rich source of information for the last ten years; similar XANES studies of nitrogen in fossil fuels have only recently been successfully performed using new, advanced fluorescence detection. Generally, the spectra of different chemical forms of nitrogen produce readily distinguishable features, thereby facilitating asphaltene analysis. Approximate contributions from different nitrogen structures present in the asphaltenes are calculated by comparing normalized areas under corresponding resonances in the spectra of the asphaltenes and the model compounds. The standard model compounds of nitrogen studied are pyrroles, pyridines, saturated amines, and metalloporphyrins. Most of the nitrogen in asphaltenes is found to be present in aromatic forms, with a very small amount as saturated amine. The pyrrole form of nitrogen is more abundant than the pyridine form in asphaltenes, and the pyridine fraction in different asphaltenes is somewhat variable. Pyridine, which is more basic than pyrrole, shows π^* resonances shifted to significantly lower energies than those observed for pyrroles. The relative positions of nitrogen π^* resonances are determined according to whether the nitrogen lone pair of electrons is shared in the π aromatic system. These spectral shifts are largely produced by resonance effects rather than inductive effects, which are observed in the sulfur case. Spectra of more complicated molecules such as porphyrins and imidazoles are explained along similar lines. The saturated amine shows only a σ^* resonance. Sensitivity of the spectra to surface effects is explored by comparing electron yield and fluoresence data.

Introduction

Asphaltenes are an important fraction of crude oil.[1] In the processing of crude oil, asphaltenes yield relatively small amounts of the most valuable hydrocarbon fractions. Asphaltenes often contain undesired heteroatoms such as sulfur and nitrogen and heavy metals such as nickel and vanadium which may poison catalysts. Physical properties of asphaltenes, such as solubility characteristics (which define asphaltenes), are important. In the production of crude oil, maintenance of formation pressures by injection of gases such as CH_4 and CO_2 can result in the in situ precipitation of asphaltenes, thereby resulting in the reduction of formation permeability. Knowledge of the chemical structures of asphaltenes is important for the optimal production and processing of crude oils. Here we use X-ray absorption near-edge structure (XANES) spectroscopy to investigate the different

structural forms of nitrogen in asphaltenes.

Asphaltenes, the heaviest component of petroleum, are dark brown or black infusible solids. They are dispersed in crude oil by association with the resins, probably in a micelle structure. Asphaltenes are defined by their solubility characteristics instead of their chemical classification;[1-3] they are insoluble in light hydrocarbons, such as *n*-heptane, but soluble in more polarizable solvents, such as benzene. Heteroatom constituents of asphaltenes play an important role in determining the solubility characteristics. In spite of their varied sources, asphaltenes generally exhibit many invariant chemical properties. Asphaltenes consist of complex macromolecules, composed principally of condensed aromatic nuclei with substituted alkyl and alicyclic systems.[1-3] The mo-

† Schlumberger-Doll Research.
‡ Lawrence Berkeley Laboratory.
§ University of California, Davis.

(1) *Chemistry of Asphaltenes*; Bunger, J. W., Li, N. C., Eds.; American Chemical Society: Washington DC, 1981.
(2) *Bitumens, Asphalts and Tar Sands*; Chillingarian, G. V., Yen, T. F., Eds.; Elsevier Scientific Pub. Co.: New York, 1978.
(3) Speight, J. G. *The Chemistry and Technology of Petroleum*; Marcel Dekker, Inc.: New York, 1980.

lecular weights of different asphaltenes vary but are approximately 5000 amu.[1-3] The H/C ratios of asphaltenes are about 1:1. Hydrogen is found predominantly in saturated groups, and 40% of the carbon atoms in asphaltenes are found in aromatic rings.[1-3]

The asphaltene fraction of a crude oil usually contains a higher percentage of heteroatoms than the original oil; the heteroatom content of asphaltenes is typically a few percent but is quite variable among different asphaltenes. X-ray absorption near-edge spectroscopy (XANES) is an effective probe of the structural forms of sulfur in asphaltenes[4,5] and coal.[6-11] Thiophene (aromatic) is the most common form of sulfur in asphaltenes, and sulfidic (saturated) sulfur is the next most abundant form.[4,5] The most common oxidized form of sulfur in asphaltenes is the sulfoxide group.[5] In coal, the most common organic form of sulfur is thiophenic sulfur, with sulfidic sulfur being the next dominant form,[7-11] and the common oxidized sulfur forms are sulfoxide, sulfone, and sulfate.[10] In lighter petroleum fractions[12] and in crude oils,[13] the most abundant form of sulfur is also aromatic thiophene.

It has been relatively difficult to study nitrogen chemistry in asphaltenes. The high molecular weights of asphaltenes impede chromatographic methods, while nonspecificity complicates many spectroscopic analyses of nitrogen. XANES spectroscopy offers a powerful and nondestructive technique for studying the nitrogen chemical structures in asphaltenes. X-ray absorption spectroscopy has been successful in the studies of N_2, revealing details of the σ_u shape resonance phenomenon.[14] High-resolution studies of N_2 showed the excitation of, in order of increasing energy, a π^* state (with resolved vibrational levels), a Rydberg series, doubly excited states, and a σ_u shape resonance.[15] Nitrogen XANES techniques have also been applied to diverse and complex chemical systems[16] such as benzothiadiazole, 1,3,2,4-benzodithiadiazine, 1,3,5,2,4-benzotrithiadiazepine, and a few polyimide complexes. Studies on nucleic acids[17] have revealed that resonances arising from 1s → π^* electronic transitions are sensitive to direct substitution at nitrogen sites, to aromatic ring disruption from exocyclic carbonyl groups, and to complementary hydrogen bonding in DNA. XANES studies on sulfur structures in fossil fuel samples have evolved for the last decade,[4-11] providing a wealth of chemical structural information of sulfur in these samples. Determination of nitrogen structures in fossil fuels by the XANES method is occurring only now. The availability of AT&T Bell Lab's high-resolution and high-flux beam line at Brookhaven National Lab and the development of multichannel soft X-ray germanium detectors have recently made nitrogen XANES studies on fossil fuel samples feasible. Additionally, nitrogen XANES requires ultrahigh vacuum techniques, unlike most sulfur XANES. We have previously reported a brief and preliminary nitrogen XANES study on a coal and a petroleum asphaltene.[18] Three model compounds were used to analyze these samples, one from each class: a pyridine, a pyrrole, and a saturated amine. These results indicated that nitrogen occurs only in aromatic forms in both of the fossil fuel samples; appreciable quantities of pyrrolic and pyridinic nitrogen were present in both cases.

In the present study, we extend our study of the nitrogen XANES spectra of petroleum asphaltenes and corresponding model compounds. Seven asphaltenes have been investigated in order to observe trends; the spectra of all the asphaltenes show three distinct resonance regions, with variations in the relative amplitudes. An extensive variety of model compounds and a large number of compounds in the important chemical classes (pyridines and pyrroles in this case) have been used to analyze nitrogen structures of the asphaltenes. All the pyridine models have spectra with π^* resonances grouped together at similar energies (400 eV) and well-separated from those of all the pyrroles, which also have their π^* resonances at similar energies (403 eV). The separation of the lowest energy π^* resonances of the pyrroles and the pyridines is explained by the orbital description of the lone pair of electrons on nitrogen. If the lone pair of electrons is shared in the π aromatic system (pyrroles), then the π^* resonances are shifted to higher energy. Correspondingly, if the lone pair is unshared (pyridines), then the π^* resonances are shifted to lower energy. This description applies to and is confirmed by spectra of more complicated molecules such as porphyrins and benzimidazole. In addition, to explore sensitivity to sample surface effects, two separate detection techniques, fluorescence detection and electron yield, have been employed. Results from the two experimental techniques are in general agreement, but some differences are noted. The XANES spectra of all the asphaltenes are similar in that three well-resolved resonance regions are observed in each spectrum, but spectral differences are also observed in terms of the resonance amplitudes. The energy of the lowest energy resonance of asphaltenes occurs in the range spanned by resonances of the pyridine models. Thus, the lowest energy resonance of asphaltenes can be correlated with pyridine analogues. Likewise, the intermediate energy resonance of asphaltenes can be correlated with pyrrole analogues. The asphaltenes as well as all model compounds exhibit a σ^* resonance. Aromatic forms of nitrogen, both pyridinic and pyrrolic, are found in significant quantities in the asphaltenes, with little evidence of saturated forms. The pyrrole content is greater than or equal to the pyridine content in all asphaltenes. Different asphaltenes show some variability in the nitrogen chemical fractions, as has been found with sulfur fractions[4,5] and unlike the more prevalent elements of asphaltenes, carbon and hydrogen.[1-3]

Experimental Section

The XANES measurements were performed at the National Synchrotron Light Source (NSLS) at Brookhaven National Laboratory on the soft X-ray ring using AT&T Bell Laboratory's "Dragon" beamline U4-B,[19] with a 600-lines/mm grating in the monochromator. Contamination with atmospheric nitrogen was avoided using high vacuum conditions in the sample chamber, generated with a cryopump and a turbo-molecular pump. The pressure in the electron beam pathway and in the sample chamber was in the range of 10^{-8}–10^{-9} Torr. The XANES spectrum of N_2 is known and does not contaminate our data. All measurements were obtained at room temperature.

A channeltron electron detector was used to acquire the electron yield data, and a multichannel germanium detector[20] was used to acquire the fluorescence yield data. The Ge detector signal was amplified using 2-μs shaping time, and the signal count rates were about 1500 counts per channel. Both detectors were used for the model compounds for con-

(4) George, G. N.; Gorbaty, M. L. *J. Am. Chem. Soc.* **1989**, *111*, 3182. Kelemen, S. R.; George, G. N.; Gorbaty, M. L. *Fuel* **1990**, *69*, 939.

(5) Waldo, G. S.; Mullins, O. C.; Penner-Hahn, J. E.; Cramer, S. P. *Fuel* **1992**, *71*, 53.

(6) Spiro, C. E.; Wong, J.; Lytle, F.; Greegor, R. B.; Maylotte, D.; Lampson, S. *Science* **1984**, *226*, 48.

(7) Huffman, G. P.; Huggins, F. E.; Shah, N.; Bhattacharya, D.; Pugmire, R. J.; Davis, B.; Lytle, F. W.; Greegor, R. B. *Processing and Utilization of High Sulfur Coals II*, Proceedings of the 2nd International Conference on Processing and Utilization of High Sulfur Coals, Carbondale, IL, 22 Sept. 28–Oct. 1, 1987; Chugh, Y. P., Caudle, R. D., Eds.; Elsevier: New York, 1987; p 3.

(8) Gorbaty, M. L.; George, G. N.; Kelemen, S. R. *Prepr. Pap.—Am. Chem. Soc., Div. Fuel Chem.* **1989**, *34*, 738.

(9) Huffman, G. P.; Huggins, F. E.; Mitra Kirtley, S.; Shah, N.; Pugmire, R.; Davis, B.; Lytle, F. W.; Greegor, R. B. *Energy Fuels*, **1989**, *3*, 200.

(10) Huffman, G. P.; Mitra Kirtley, S.; Huggins, F. E.; Shah, N.; Vaidya, S.; Lu, F. *Energy Fuels*, **1991**, *5*, 574.

(11) Gorbaty, M. L.; George, G. N.; Kelemen, S. R. *Fuel* **1990**, *69*, 1065.

(12) Terell, R. E., et al. *Anal. Chem.* **1983**, *55*, 245R.

(13) Waldo, G. S.; Carlson, R. M. K.; Moldowan, J. M.; Peters, K. E.; Penner-Hahn, J. E. *Geochim. Cosmochim. Acta* **1991**, *55*, 801.

(14) Dehmer, J. L.; Parr, A. C.; Southworth, S. H. *Handbook on Synchrotron Radiation*; Marr, G. V., Ed.; 1987; p 241.

(15) Chen, C. T.; Ma, Y.; Sette, F. *Phys. Rev. A* **1989**, *40*, 6737.

(16) Schedel-Niedrig, Th.; Keil, M.; Sotobayashi, H.; Schilling, T.; Tesche, B.; Bradshaw, A. M. *J. Phys.: Condens. Matter* **1991**, *3*, S23. Schedel-Niedrig, Th.; Keil, M.; Sotobayashi, H.; Schilling, T.; Tesche, B.; Bradshaw, A. M. *Int. J. Phys. Chem.* **1991**, *95*, (11), 1385. Johnson, A. L.; Muetterties, E. L.; Stöhr, J.; Sette, F. *J. Phys. Chem.* **1985**, *89*, 4071.

(17) Mitra Kirtley, S.; Mullins, O. C.; Chen, J.; van Elp, J.; George, S.; Chen, C. T.; O'Halloran, T.; Cramer, S. P. *Biochem. Biophys. Acta.* In press.

(18) Mitra Kirtley, S.; Mullins, O. C.; van Elp, J.; Cramer, S. P. *Fuel.* In press.

(19) Chen, C. T. *Nucl. Instrum. Methods Phys. Res., Sect. A* **1987**, *256*, 595. Chen, C. T.; Sette, F. *Rev. Sci. Instrum.* **1989**, *60*, 1616.

(20) Cramer, S. P.; Tench, O.; Yocum, M.; Kraner, H.; Rogers, L.; Radeka, V.; Mullins, O. C.; Rescia, S. *X-Ray Absorption Fine Structure*, Proceedings of the 6th International XAFS Conference; Hasnain, S. S., Ed.; Ellis Horwood: Chichester, 1991; p 640.
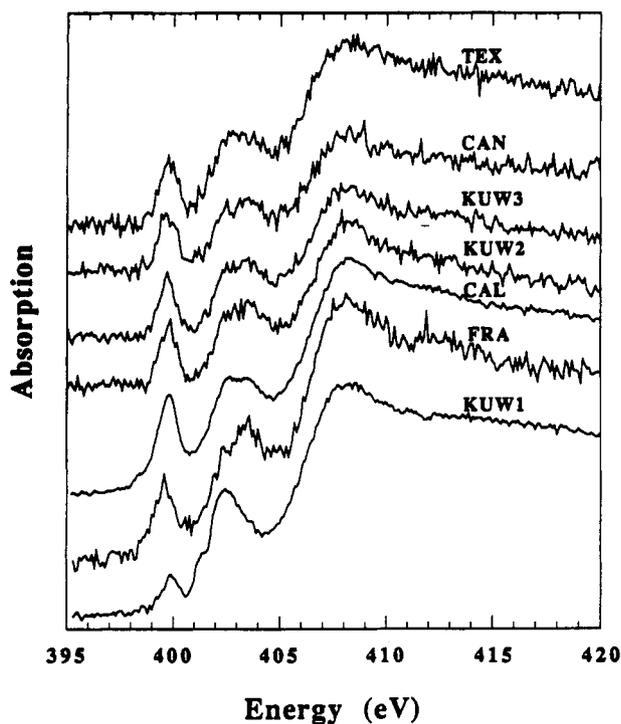
Figure 1. Fluorescence yield XANES spectra of seven asphaltene samples: TEX, CAN, KUW3, KUW2, CAL, FRA, and KUW1. Each spectrum exhibits three well-resolved resonance regions.

sistency check. In order to avoid surface effects often observed in electron yield data, fluorescence yield data were collected for all asphaltenes. In order to investigate any sensitivity of the data to different detection methods, both methods were employed to obtain data of several samples.

The asphaltenes were prepared by n-heptane precipitation from crude oils obtained from California (CAL), Kuwait (KUW1, KUW2, and KUW3), France (FRA), Canada (CAN), and Texas (TEX), and the preparation method has been described elsewhere.[21]   The suite of standard samples studied consists of five pyridine samples (acridine, poly(4-vinylpyridine-co-styrene), phenanthridine, 4,7-phenanthroline, and 2,6-di-p-tolylpyridine), four analogues of pyrrole (carbazole, tetrahydrocarbazole, poly(9-vinylcarbazole), and 2-phenylindole), a saturated amine (1,3,5-tribenzylhexahydro-1,3,5-triazine), two porphyrin samples (5,10,15,20-tetraphenylporphyrinvanadium(IV) oxide and 2,3,7,8,12,13,17,18-octaethylporphyrinnickel(II), and an imidazole analogue (2-methylbenzimidazole). All the model compounds were obtained from Aldrich Chemical Company and were used without further purification.

Samples of asphaltenes were mounted for X-ray spectroscopy by two different methods. Asphaltenes CAL, FRA, and KUW1 were dissolved in CCl$_4$, and films of these solutions were then made by evaporation on small silicon wafers. These wafers were mounted on a gold-plated sample holder by means of silver epoxy. The rest of the asphaltene samples and the model compounds were first ground with a mortar and pestle and then mounted on the gold-plated sample holder on small strips of nitrogen-free double sticking tape. It was found that the asphaltene samples mounted on the nitrogen-free tape produced better electron yield data than asphaltene samples evaporated on silicon wafers. Elemental analysis (% by wt) showed that[22] CAL contains 82.91% C, 8.55% H, 2.32% N, 2.60% S, 3.75% O, 141 ppm V, and 632 ppm Ni; FRA contains 90.79% C, 7.53% H, 0.54% N, 0.68% S, 1.11% O, 2.6 ppm V, and 8.5 ppm Ni; KUW1 contains 79.20% C, 7.82% H, 0.98% N, 7.61% S, 2.45% O, 438 ppm V, and 141 ppm Ni; KUW2 contains 81.34% C, 7.57% H, 0.85% N, 8.84% S, and 0.87% O; KUW3 contains 83.28% C, 8.04% H, 0.95% N, 7.76% S, and 0.98% O; and CAN contains 84.30% C, 8.12% H, 0.91% N, 5.82% S, and 1.42% O.

Results and Discussions

Figure 1 plots the nitrogen K-edge XANES fluorescence excitation spectra of seven different asphaltene samples, TEX, CAN, KUW3, KUW2, CAL, FRA, and KUW1. Each spectrum fea-

tures three distinguishable and well-resolved resonance regions. The first resonance occurs around 399.3–399.8 eV, followed by one or two slightly broader features between 402 and 403 eV; the third region consists of a more intense and broad resonance at around 408.3 eV. A few overlapping, broader resonances are often present at higher energies. Generally the nitrogen XANES spectra of the different asphaltenes are similar, but some variability is noted, particularly in the magnitudes of the first resonance.

Figure 2 compares the fluorescence yield XANES spectra of the asphaltene CAL with those of four standard compounds (the corresponding chemical structures of models are shown next to the spectra). The sharp low-energy peaks (399 eV < E < 405 eV) represent electronic transitions from 1s to different π^* levels, and the broader resonances at higher energies ($E \approx$ 407–409 eV) correspond to σ^* shape resonances.[23]   It is clear from Figures 1 and 2 that, as in all seven asphaltene spectra, each resonance region in the spectrum of CAL matches with the first (major) resonance (π^* or σ^*) region of the XANES of a particular nitrogen structure. For example, the lowest-energy resonance of CAL matches the first (π^*) resonance of acridine, which is a pyridine analogue, thereby suggesting contribution of the pyridine structure in the asphaltene. Likewise, the second resonance region in the CAL XANES spectrum (402.5–403.3 eV) shows contributions from pyrrole molecules such as carbazole. At 408 eV, the asphaltene spectrum shows a large resonance. All model compounds exhibit a σ^* shape resonance near this energy. The saturated amine hexahydrotriazine, however, exhibits only the shape resonance at 407.3 eV; it has no π^* resonance. Therefore, the signature of a saturated amine in the asphaltene spectra would correspond to a large shape resonance and the absence of π^* resonances.

Figure 2 also illustrates the sensitivity of the XANES features of the model compounds to different chemical structures. The pyridine analogue acridine shows a π^* resonance at a considerably lower energy ($\Delta E \approx$ 3 eV) than the π^* resonance of a pyrrole analogue (carbazole). In a pyridine molecule, the lone pair of electrons at the nitrogen site is unshared in an sp^2 orbital, and the electronegative nitrogen possesses greater electron density than neighboring carbon sites. In contrast, the lone pair of electrons at the nitrogen site in pyrrole is shared in the aromatic π cloud of the five-membered ring system. As a consequence, there is a net positive charge left on the nitrogen site of a pyrrole molecule; thus, pyridine is much more basic than pyrrole. Therefore, the lowest energy π^* resonance in the XANES spectrum of pyridine shifts to lower energy relative to the lowest energy π^* resonance of pyrrole. Similar phenomena have been observed before: studies on molybdenum[24] have revealed a linear correlation between the coordination charge, ranging from 0 to +5, of a series of molybdenum compounds and the shift in the X-ray absorption edge of the respective spectra. Higher (positive) oxidation states result in an increase in the energy of XANES resonances. Similar studies on different vanadium oxides[25] have shown that there is a blue shift in the vanadium X-ray absorption edge with an increase of the formal oxidation number of vanadium (enhanced net positive charge on vanadium). X-ray absorption studies on a series of sulfur compounds with differing oxygen substitution have also shown similar phenomena.[4,5,9–11] The positions of the sulfur 1s → 3p peak in the XANES spectra of various oxidized and reduced sulfur compounds vary over a large range (~11 eV) with a change of oxidation number from -1 to +6, and the greater the oxidation state, the higher the energy.[4,5,9–11]

There are, nevertheless, significant differences in the interpretation of XANES spectra between sulfur and nitrogen compounds. In nitrogen XANES spectra, covalent effects are much more prominent than in sulfur XANES spectra. In the simplest picture, the sulfur spectra can be described in terms of atomic orbitals, whereas the nitrogen spectra must be described in terms

(21) Mullins, O. C. *Anal. Chem.* **1990**, *62*, 508.

(22) Elemental analyses on asphaltenes performed by Galbraith Laboratories, Knoxville, TN.

(23) Stohr, J.; Jaeger, R. *Phys. Rev. B* **1982**, *26*, 4111. Dehmer, J. L.; Dill, J. *J. Chem. Phys.* **1976**, *65*, 5327.

(24) Cramer, S. P.; Eccles, T. K.; Kutzler, F. W.; Hodgson, K. O.; Mortenson, L. E. *J. Am. Chem. Soc.* **1975**, *98:5*, 1287.

(25) Wong, J.; Lytle, F. W.; Messmer, R. P.; Maylotte, D. H. *Phys. Rev. B* **1984**, *30* (10), 5596.
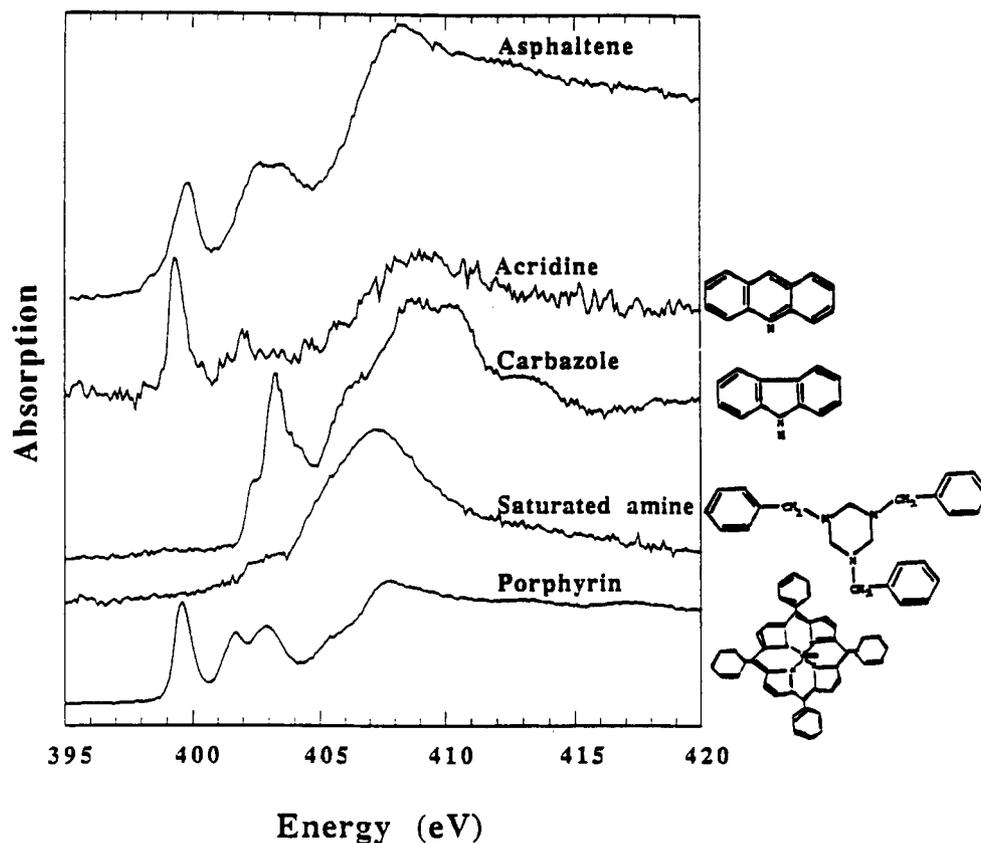
Figure 2. Fluorescence yield XANES spectra of asphaltene CAL and four different nitrogen model compounds. The spectra of the model compounds have been corrected for thickness effects using procedures described in the text. The spectral correlation between the different nitrogen model compounds and asphaltene is evident. The first two features in the asphaltene spectrum correspond to the π^* resonances of the spectra of pyridine and pyrrole, signifying contributions of these structures to asphaltene. The spectrum of pyrrole shows a blue-shifted π^* resonance compared to the π^* resonance of pyridine. Porphyrin content in the asphaltenes is assumed to be given by the (small) vanadium and nickel content of the asphaltenes.

of molecular orbitals. The sulfur XANES spectra are characterized by a single large resonance (1s → 3p), where the peak position and magnitude are determined by the formal oxidation state of sulfur.[4,5,9-11] Nitrogen XANES spectra exhibit π and σ resonances, and the location of nitrogen π resonances are governed not by formal oxidation state but rather by complexities associated with covalent bonding.

In the nitrogen case, the large separation between pyrrole and pyridine π^* resonances makes it straightforward to discern the relative contributions from these two nitrogen types in asphaltenes. Shorter bond lengths have been found to correlate nearly linearly with higher energy for σ shape resonances.[26] In our case, the C–N bond length in pyrrole ($\sim$1.39 Å) is greater than that of pyridine ($\sim$1.34 Å),[27] and the π^* position of pyrrole is at a higher energy than that of pyridine. This indicates that the bond lengths do not correlate in any simple manner with the positions of the π^* resonances.

Many pyridine and pyrrole analogues have been investigated here in order to verify that (1) the arguments we have developed to understand peak positions apply generally to nitrogen-containing aromatic molecules and that (2) the peak positions of the asphaltene spectra are located within the energy range spanned by pyridine (and pyrrole) analogues. Figure 3 shows the fluorescence yield XANES spectra of four different pyrrole and four different pyridine analogues (some chemical structures are shown). The pyridine analogues are significantly different in chemical structure; nevertheless, their lowest energy resonances are quite close to each other, spanning a range of $\sim$0.7 eV. Furthermore, the lowest energy resonances of the asphaltenes are found within the same energy range spanned by the pyridine analogues. Likewise, the

pyrrole analogues represent distinctly different chemical structures. As with the pyridine analogues, the lowest energy resonances of the pyrrole analogues are found in a small energy range (although 2-phenylindole does show additional structure, perhaps due to a splitting). Again, the intermediate energy resonances of the asphaltenes are found within the range spanned by the pyrrole analogues. Thus, we conclude that our arguments regarding the relative positions of π^* resonances for pyrroles and pyridines are accurate. Furthermore, the fact that resonance energies of the asphaltenes and models match is a reassurance that our analysis of asphaltenes using pyrrole and pyridine models is correct. Perhaps XANES spectra which are more resolved would allow for individual molecular components or subsets of molecular classes to be identified in asphaltenes. The broad π^* resonances in the spectra of asphaltenes, particularly in the second (pyrrole) resonance region, are probably due to the presence of a variety of chemical structures of particular analogues in asphaltenes.

It is instructive to determine whether correlations of peak positions with nitrogen type extend to more complicated molecules. Figure 4 shows the fluorescent yield spectra of nickel octaethylporphyrin and methylbenzimidazole. Free-base octaethylporphyrin produces a spectrum similar to that of nickel octaethylporphyrin but with the resonances shifted to lower energy by $\sim$1 eV. Both spectra of Figure 4 exhibit π^* resonances in two distinct spectral ranges, one close to the pyridine lowest energy π^* resonance energy and the other close to the pyrrole lowest energy π^* resonance energy. Imidazole contains two nitrogens; one nitrogen has a lone pair in the p_z orbital, which is involved in the aromatic system (pyrrolic nitrogen), and the other nitrogen has its lone pair unshared in an sp^2 orbital (pyridinic nitrogen). It appears that each of the two nitrogens in benzimidazole produces a particular resonance according to the nitrogen type. Similarly, porphyrins also contain two types of nitrogen, pyrrolic and pyridinic, and correspondingly exhibit both pyrrolic and pyridinic

(26) Sette, F.; Stöhr, J.; Hitchcock, A. P. *Chem. Phys. Lett.* **1984**, *110*, 517. Stöhr, J.; Sette, F.; Johnson, A. L. *Phys. Rev. Lett.* **1984**, *53*, 1684.
(27) Dewar, M. J. S.; Gleicher, G. J. *J. Chem. Phys.* **1966**, *44* (2), 759.
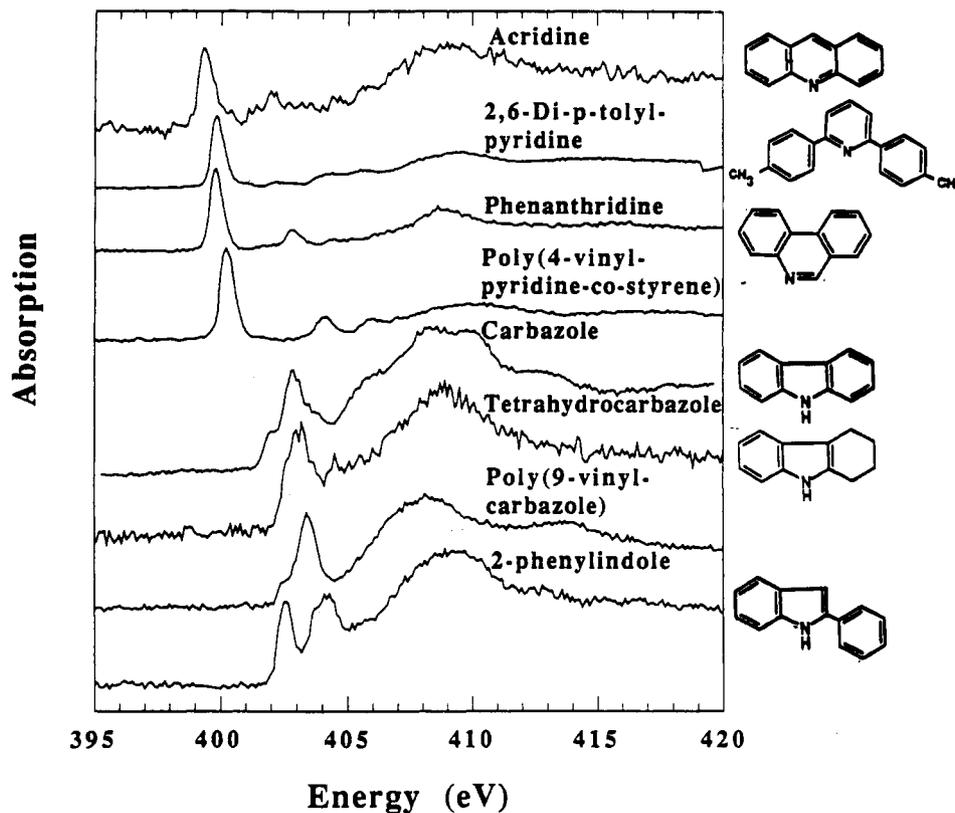
Figure 3. Fluorescence yield XANES spectra of four different pyrrole and four different pyridine analogues. These spectra have been corrected for thickness effects using procedures described in the text. Some chemical structures are given next to the corresponding spectrum. As a result of changes in the chemical structures of pyrroles, the π^* resonances of their spectra vary within 0.5 eV of each other; the same is true for the spectra of the pyridines. The first (π^*) resonances of the pyrrole analogues occur at energies well-separated ($\Delta E \approx 3$ eV) from those of the pyridine analogues. Alkyl substitution at the nitrogen site in the poly(9-vinylcarbazole) does not produce any significant changes in the XANES spectrum.
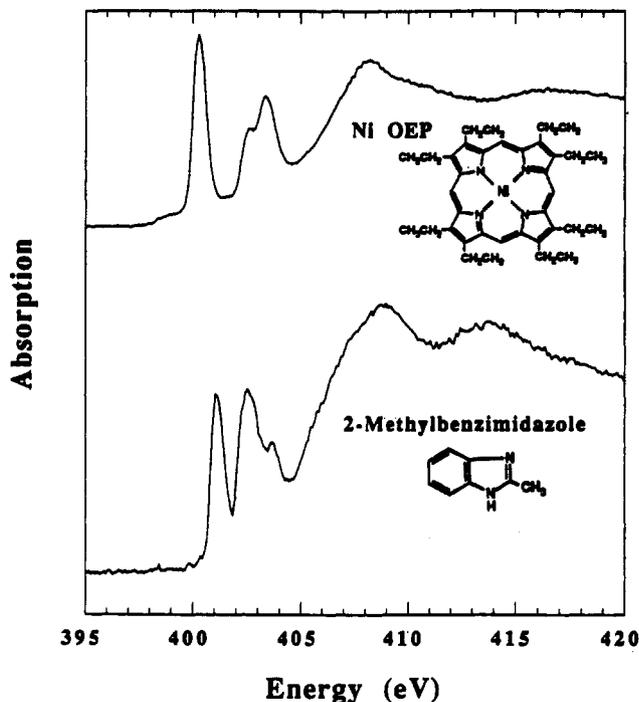
Figure 4. Fluorescence yield spectra of nickel octaethylporphyrin and of 2-methylbenzimidazole. Each spectrum shows two distinct peaks, the lower energy peak in the pyridine range and the higher energy peak in the pyrrole range.

Table I. Percentages of Different Nitrogen Structures in Asphaltenes[a]

asphaltene sample	approximate contributions, in %, from different nitrogen structures			
	pyrrole	pyridine	saturated amine	porphyrin[b]
TEX	80	18	0	
CAN	74	26	0	
KUW3	77	22	2	
KUW2	79	22	0	
KUW2[c]	71	26	3	
CAL	65	30	2	3
FRA	76	22	3	0.2
KUW1	87	2	2	7

[a] Obtained from the fluorescence yield spectra unless otherwise stated. [b] Determined from the metal content of the asphaltenes. [c] Obtained from electron yield spectra.

and benzimidazole, it appears that the dominant determinant in the position of π^* resonances is the type of nitrogen, pyrrolic or pyridinic. The number of atoms in the aromatic ring does not govern nitrogen type; rather, it is the orbital description of the lone pair. Multiple heteroatoms in a single aromatic ring can result in some shifts in peak positions, as seen in the methyl benzimidazole spectrum. However, the lowest energy peak of the spectrum of 4,7-phenanthroline (not shown) is at 399.7 eV; this compound has two pyridinic nitrogen sites in different rings.

A least-squares fitting program was employed on the XANES spectra of the entire suite of samples. The resonance widths in the spectra of the asphaltenes are greater than the peak widths in the spectra of the model compounds; therefore, instead of fitting the asphaltene spectra with a sum of spectra of model compounds, each individual spectrum of the asphaltenes and model compounds was fitted. Each spectrum was fitted with a superposition of several Lorentzian peaks and an arctangent step function. The step function denotes the electronic transition to the continuum,

resonances. The actual wave function of a metalloporphyrin may be such that each nitrogen atom has pyrrolic and pyridinic character, but this apparently does not significantly influence the XANES spectrum. From examination of the spectra of porphyrins
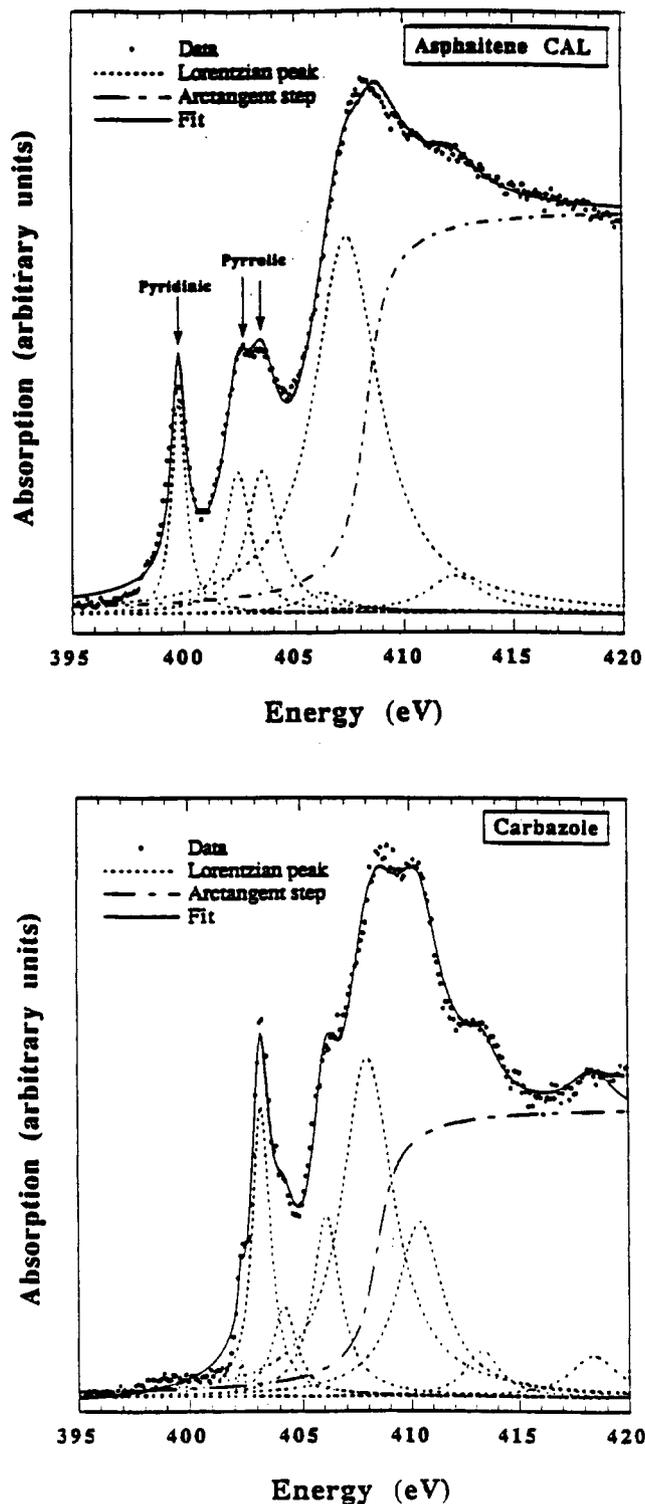
Figure 5. Typical least-squares fits of fluorescence yield spectra of an asphaltene (CAL) and a model compound (carbazole). The fitting routine was based on fitting the data with the sum of a number of Lorentzian resonances and an arctangent step function.

while the peaks represent resonance transitions. Figure 5 shows fitted fluorescence yield spectra of a model compound and an asphaltene sample. The fitting analysis was performed on a Macintosh computer, using KaleidaGraph software. In all the fitting routines, the position ($E \approx 408.5$ eV) and the width (~ 1.5 eV) of the step function were constrained to have similar values for all the samples. The area under each peak of the sample was determined and then normalized with respect to the corresponding step height. Thickness (concentration) effects in the fluorescence excitation spectra of the standard compounds are small ($<10\%$)

and have been corrected for using tables of atomic subshell photoionization cross-sections for carbon, nitrogen, and oxygen[28] and a correction formula described elsewhere,[29] in a similar manner as performed in the case of sulfur;[5,13] the corrected spectra have been used in the final analysis procedures. The correction is smaller for models with lower concentrations of nitrogen. The thickness effects in 4,7-phenanthroline were deemed higher than acceptable, so this compound was not included in the final analysis.

The percentages of the different nitrogen compounds present in the asphaltene samples were then calculated. After the porphyrin contribution was subtracted (see details below) from the first peak area of an asphaltene spectrum, the remainder of the area was attributed to pyridine analogues. Considerable variability is observed between the ratios of π^* resonance areas to step heights in the spectra of different pyridine analogues. This ratio in the spectrum of poly(4-vinylpyridine-co-styrene), for example, is about 2.5 times larger than the same ratio in the spectrum of acridine (Figure 3). This variability produces uncertainty in the estimation of the pyridine content. In contrast, the spectra of the pyrrole analogues exhibit similar ratios of peak areas to step heights (Figure 3). The first resonance region of each asphaltene spectrum was attributed to equal weights of the four pyridine analogues; by matching the normalized areas of the first resonance region in the asphaltene spectrum with the corresponding resonances in the pyridine spectra, the pyridine contribution in the asphaltene sample was determined. The second resonance region of an asphaltene spectrum was attributed to equal weights of the four pyrrole analogues after contributions of pyridine and porphyrin spectra to this resonance area were subtracted. An average contribution from the pyrrole type of nitrogen in the asphaltenes was then calculated. After contributions from the spectra of porphyrin, pyridine, and pyrrole were subtracted from the σ^* shape resonance region of the asphaltene spectrum ($E \simeq 408$ eV), the remainder of this resonance area was attributed to saturated amine.

Petroleum and asphaltenes are known to contain small quantities of metalloporphyrins complexed with vanadyl and nickel ions.[3] The porphyrin fraction was calculated by first determining the quantity of vanadium and nickel in the asphaltenes.[22] We then assumed that all vanadium and nickel are complexed in porphyrin structures; this procedure provides a calculated porphyrin fraction of the asphaltene, and by knowing the nitrogen concentration the porphyrin nitrogen fraction can be computed. This procedure was performed on only three asphaltenes, because the resulting porphyrin fraction was determined to be small and possibly overestimated because some of the vanadium and nickel may not be complexed with porphyrin.[30] The small value of the porphyrin fraction is consistent with the lack of a Soret band in the visible absorption spectrum of these asphaltenes.[31] The porphyrin spectral contribution was subtracted from the asphaltene spectra in the analysis procedure.

Table I lists the calculated nitrogen fractions in the asphaltenes. Most of the nitrogen in these asphaltenes is aromatic, and, of the aromatic, pyrrolic nitrogen is more abundant than the pyridinic type. Out of seven samples, five asphaltenes are fairly similar in their pyrrole and pyridine fractions, while two are different. Asphaltene KUW1 also has the smallest pyridine fraction, consistent with the fact that the XANES spectrum of this asphaltene has the smallest first (pyridine) resonance (Figure 1). An overestimation of the porphyrin fraction would lead to our underestimating the pyridine fraction; regardless, the pyridine fraction of this asphaltene is low. For KUW1, the low pyridine fraction coupled with the emergence of a large peak at 402 eV may indicate that the pyridine has been chemically modified, perhaps oxidized, in this sample, producing a different nitrogen type with absorption at 402 eV. One plausible reason for the presence of pyrrolic nitrogen in asphaltenes is that pyrrolic compounds are produced

(28) Yeh, J. J.; Lindau, I. *Atomic Nuc. Data Tables* **1983**, *32*, 1.
(29) Equation 23 described by J. Goulon; Goulon-Ginet, C.; Cortes, R.; Dubois, J. M. *J. Phys.* **1982**, *43*, 539.
(30) Fish, R. H.; Komlenic, J. J.; Wines, B. K. *Anal. Chem.* **1984**, *56*, 2452.
(31) Mullins, O. C.; Zhu, Y. *Appl. Spectrosc.* **1992**, *46*, 354.
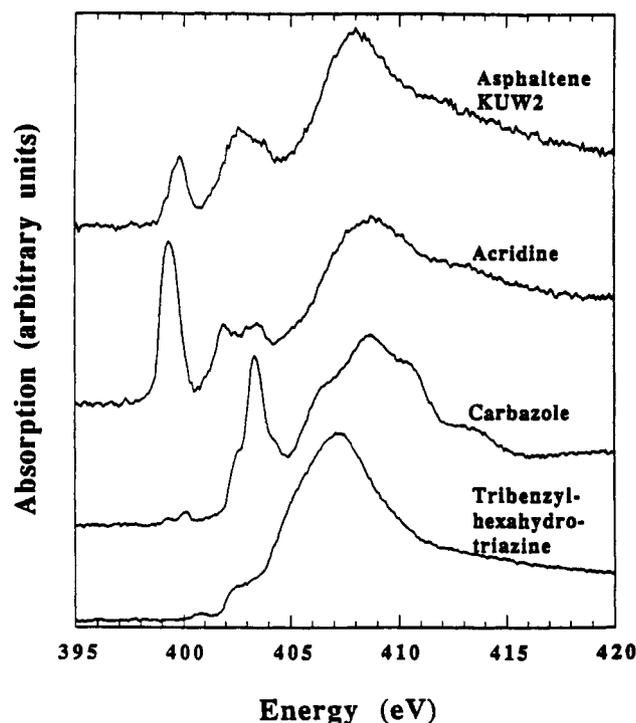
Figure 6. Electron yield XANES spectra of an asphaltene and a few model compounds. The analysis performed on the electron yield spectrum of the asphaltene was similar to that performed on the fluorescent yield spectrum and gave comparable results.

in the degradation of chlorophyll, a source material for crude oil. Table I lists uniformly small fractions of saturated amines in all asphaltenes. The porphyrin fractions of the asphaltenes whose metal analyses have not been performed are assumed to be low, as with the other asphaltenes. The total fractions of nitrogen were normalized to add to 1; the normalization constant generally was near 1. It should be noted here that, as with sulfur,[4,5] the most prevalent form of nitrogen in asphaltenes is found in aromatic rings. Variability of the different structures of sulfur has been observed in the asphaltenes, similar to nitrogen. However, in contrast to nitrogen structures, significant fractions of saturated forms of sulfur are also found in asphaltenes. Carbon also occurs both in aromatic and saturated forms in asphaltenes.

N 1s X-ray photoemission spectroscopy (XPS) studies have previously been performed on a suite of coals[32,33] and several samples of raw coals and coal-derived materials such as asphaltenes.[34] In this case, the separation of the peaks in the XANES data of pyrroles and pyridines (ΔE at least 2.3 eV) is found to be much larger than the peak widths ($\sim$1.5 eV), whereas in the XPS results on coal and coal-derived materials the peak separations ($\Delta E \approx 1.4$–2 eV) are comparable to peak widths ($\sim$2 eV). XPS results indicate that the coal asphaltenes[34] contain 49–62% of pyrrolic nitrogen and coals[32] 65–85% of pyrrolic nitrogen, with the remaining nitrogen assigned to pyridine fractions in both cases. These results are similar to our earlier XANES results for a coal and a petroleum asphaltene.[18]

In order to investigate the sensitivity of the data to possible surface effects, electron yield detection as well as fluorescence detection was performed on a series of samples. Figure 6 shows the electron yield spectra of asphaltene KUW2, acridine, carbazole, and saturated amine. Comparison of Figures 1, 2, and 6 reveals that the electron yield data of the models and the asphaltene have enhanced ratios of peak intensities to step heights relative to fluorescence spectra. Note that the fluorescence spectra of the models have been corrected for sample thickness effects. Fur-

thermore, for samples as dilute in nitrogen as asphaltenes, it is difficult to imagine significant sample thickness effects. An analysis procedure involving the fluorescent data of the asphaltenes and the electron yield data of the models would, therefore, produce erroneous results. Thus, fluorescence results of the standard compounds were used to analyze the fluorescence excitation spectra of asphaltenes; likewise, electron yield spectra of the model compounds were used to analyze the electron yield spectra of the asphaltene KUW2. The least-squares analysis discussed before was performed on the electron yield spectrum of asphaltene KUW2, using normalized area ratios obtained from the electron yield spectra of the standard compounds, and the results are listed in Table I. The similarity in the analysis of fluorescence results and electron yield results implies that surface effects are not a significant problem; the two sets of results agree within 10% of each other, thereby providing an error estimate. The conclusion that surface effects are not significant for these types of samples agrees with previous XPS results.[33] The porphyrin percentage in this sample has not been calculated and is assumed to be small, as in the other asphaltenes studied here. Variation of the amplitudes of peak resonances with respect to step heights was observed in many standard compounds, especially in the case of pyridine analogues. We have seen that this variability in peak amplitudes does result in increased uncertainty; we assign an error of 12% to the nitrogen percentages listed in Table I.

Electron yield data, unlike fluorescence data, are sensitive to surface effects. In addition to this, fluorescence and electron yield data differ in several other aspects: fluorescence emission and detection are anisotropic, as is evident from orientation studies on surfaces,[16] whereas electron yield measurements are isotropic. Furthermore, there is a possibility that the ratio between Auger electron emission and fluorescence emission is affected by excitation of (quasi) bound resonances, which would result in variations between electron yield and fluorescence spectra. It is also possible that there are different branching ratios among the different fluorescent decay channels, giving rise to differential self-absorption with fluorescence detection. Thus, it is difficult to determine the cause of differences in corresponding spectra between Figures 2 and 6.

Conclusions

XANES has proven successful in the investigation of the different forms of nitrogen in petroleum asphaltenes. XANES spectra of the asphaltenes have distinguishable, well-separated resonances, which can be well accounted for using a large suite of model compounds. Thus, the fractions of different chemical classes of nitrogen in asphaltenes can be readily discerned. Most of the nitrogen in asphaltenes is aromatic; pyrrole and pyridine structures are the most prevalent forms of nitrogen in asphaltenes. Pyrrolic nitrogen is more abundant than pyridinic forms, and some variability among the pyrrole and pyridine fractions is observed in the asphaltenes. Contributions from saturated amines are found to be negligible. XANES resonance positions of aromatic nitrogen are determined by the nitrogen type; pyridinic compounds have lower energy π^* resonances than pyrrolic compounds. The relative positions of the resonance energies are explained on the basis of the molecular orbital description of the lone pair of electrons at the nitrogen site. XANES spectra of complex molecules containing both pyridinic and pyrrolic nitrogen sites, such as porphyrins and benzimidazole, also exhibit pyridinic and pyrrolic resonances and can be explained accordingly. Electron yield and fluorescence yield results are in reasonable agreement, suggesting that surface effects are not significant for asphaltene spectra.

(32) Burchill, P. *Proceedings of the International Conference on Coal Science*; Moulijn, J. A., et al., Eds.; Elsevier Science Publ. B. V.: Amsterdam, 1987.
(33) Burchill, P.; Welch, L. S. *Fuel* **1989**, *68*, 100.
(34) Wallace, S.; Bartle, K. D.; Perry, D. L. *Fuel* **1989**, *68*, 1451.